Household slow sand filter efficiency with *schmutzdecke* evaluation by microsensors

Antonio Wagner Lamon[a]; Paulo Marcos Faria Maciel[a]; José Roberto Campos[a]; Juliano José Corbi[a]; Patrick Stuart Morris Dunlop[b]; Pilar Fernandez-Ibañez[b]; John Anthony Byrne[b]; Lyda Patricia Sabogal-Paz[a*]

[a]Department of Hydraulics and Sanitation, São Carlos School of Engineering, University of São Paulo, Avenida Trabalhador São-Carlense 400, São Carlos, São Paulo, 13566-590, Brazil.

[b]Nanotechnology and Integrated Bioengineering Centre, School of Engineering, Ulster University, Jordanstown, BT37 0QB, Northern Ireland, United Kingdom.

* Corresponding author: lysaboga@sc.usp.br

ABSTRACT

Slow sand filtration is a common technology providing potable water in rural households across Latin America, Asia and Africa. Two PVC household slow sand filters (HSSF) were operated in continuous (C-HSSF) and intermittent (I-HSSF) flow modes for eight consecutive months. A non-woven blanket was installed on the fine sand top to facilitate cleaning with scheduled maintenance undertaken every 30 days. The efficiency of each HSSF was evaluated via physico-chemical indicators (reduction of turbidity and colour) with biological performance assessed via total coliform and *E. coli* enumeration post treatment. There were no statistically significant differences between the continuous flow and intermittent flow models for physical-chemical and total coliform reduction parameters. However, when evaluating *E. coli*, C-HSSF performed better (p = 0.02). The non-woven blanket was subjected to weekly analysis using a

Clark-type amperometric microsensor (diameter < 20 µm), which measured dissolved oxygen (DO) concentration in the adherent biofilm. DO microprofiles illustrated a variation in biofilm growth, which were associated with a progressive increase in the HSSF efficiency. The maximum DO depletion value measured during several months of operation showed no significant difference between I-HSSF and C-HSSF (p=0.98). The microsensor measurements provided unprecedented results in real time. These results can help to understand the efficiency of the filter in relation to the biofilm growth, the dissolved oxygen depletion and turbidity removal.

Keywords: dissolved oxygen, drinking water, rural communities, biofilms, tracer tests, slow sand filters

Abbreviations:

HSSF: household slow sand filter

C-HSSF: household slow sand filter in continuous flow

I- HSSF: household slow sand filter in intermittent flow

SSF: slow sand filter

1. INTRODUCTION

The World Health Organization reports that more than 800 million people live in precarious situations regarding availability of safe and affordable drinking water (WHO, 2017). In order to address this problem primarily within developing countries, a solid base for drinking water treatment technologies is required. Conventional systems used in cities and developed

countries are complex and expensive, and consequently basic water treatment technologies are being adapted to local contexts worldwide (Sianipar et al., 2013).

Point-of-use (POU) devices treat water for direct consumption (drinking and cooking) and are an option for water supply where conventional water treatment plants are not affordable (USEPA, 2006). Among the most prevalent POU interventions is the household slow sand filter (HSSF) in intermittent flow, with more than 300,000 units installed (CAWST, 2012). The filter body can be made of concrete or plastic and the bed is made of fine sand and gravel. The simplified configuration enables the production of safe water to low-cost, with a filter that is easy-to-build, durable and efficient, widely used in developing countries (CAWST, 2012; Mahaffy et al., 2015).

HSSFs can provide an effective treatment for the removal of physico-chemical and microbiological parameters present in water (Stauber et al., 2006; Gottinger et al., 2011). According to Saravanan & Gobinath (2015), HSSFs can remove 5.0-64% of metals and 90-99% of turbidity, however their efficiency is limited to the use of raw water with turbidity below 50 NTU (CAWST, 2012). Sabogal-Paz et al (2020) reported that raw water turbidity should be limited to 10 NTU in countries with higher drinking water standards.

Developing countries usually have raw water with high turbidity levels (Clair, 2009; Shaikh & Munavalli, 2015) with several studies reporting adjustments in the HSSF operational parameters and related efficiency to the quality of produced drinking water (Kennedy et al. 2012; Young-Rojanschi & Madramootoo, 2014; Young-Rojanschi and Madramootoo, 2015; Souza Freitas and Sabogal-Paz, 2019; Terin and Sabogal-Paz, 2019; Maciel & Sabogal-Paz, 2020; Sabogal-Paz et al 2020).

In such filters, the fine sand layer remains immersed in water permitting the formation of a biofilm (i.e. *schmutzdecke*), which imposes greater head loss as the resultant filter efficiency increases. *Schmutzdecke* formation is important with respect to filter performance

(Kristina et al., 2015), and given that the reactions inside the biofilm are predominantly aerobic, a better understanding of both dissolved oxygen (DO) distribution and *schmutzdecke* formation is crucial for slow sand filter (SFF) efficiency. Although studies on HSSF have focused on operational parameters and efficiency, the biofilm and its effective contribution to water purification have not been widely evaluated.

1.1. HSSFs in continuous and intermittent flows

HSSF in continuous flow (C-HSSF) is commonly used with 0.20-1.22 $m^3m^{-2}day^{-1}$ filtration rate (Young-Rojanschi and Madramootoo, 2014; Souza Freitas and Sabogal-Paz, 2019), which must be controlled daily by a valve. According to Sabogal-Paz et al. (2020), such a filter can produce ≤ 200 L per day when supplied by an elevated tank or pump, occupying a larger area inside a house when compared to HSSF operated with intermittent flow (I-HSSF). Young-Rojanschi and Madramootoo (2014) observed that C-HSSF can be more efficient in *E. coli* reduction (3.71 log) than I-HSSF (1.67 log), with initial values of 410 ± 60 CFU/100 mL in raw water. On the other hand, turbidity removal was around 87-96% from the initial 12.6 ± 7.3 NTU measured in influent water.

I-HSSF can operate with filtration rates ≤ 9.6 $m^3m^2day^{-1}$ (CAWST, 2012). The filter is fed in sequential batches, thus water remains inside for 1-48 h (i.e. buffer period), allowing the filtration processes to treat water (CAWST, 2012). I-HSSF occupies a smaller area in a residence (Sabogal-Paz et al., 2020) and can produce ≤ 80 L per day (Schmidt and Cairncross, 2009). According to Elliott et al. (2008), I-HSSF can achieve 74.8% of turbidity removal (initial value: 1.86-8.96 NTU) with a reduction of 0.5-1.9 log of *E. coli* (initial value: 255 ± 33 CFU/100mL).

1.2. Biological layer (biofilm)

Biofilms are complex structures with dynamic systems that favour primordial multicellular organisms and ecosystems of varied characteristics (Hall-Stoodley, 2004). Biofilm adhesion is a complex process regulated by the characteristics of the substrate, temperature, hydrodynamics, and other factors. A biofilm is comprised of microbial cells and extracellular polymeric substances (EPS) and its defined architecture provides an adequate environment for the exchange of genetic material among cells (Donlan, 2002).

Microorganisms present in biofilms come from raw water and form a community comprising algae, bacteria, protozoa, and small living cells (Pfannes et al., 2015; Prem and Manjeet, 2018). The microorganisms and their variety of species adapt to the raw water characteristics, as well as to the SSF environment (Buzunis, 1995).

Raw water quality is important for the microbiological community and maintenance of its metabolism in the biofilm. Oxidative processes during metabolism consume organic matter in raw water, including dead pathogens. Microorganisms compete for food and with more space in the biofilm; metabolic rates increase considerably, particularly at higher temperatures (Prem and Manjeet, 2018).

Huisman and Wood (1974) identified the microbiological process of water purification in the SSF sand (i.e. the first 40 cm below the biofilm). The biochemical reactions, in this biological layer, gain space by converting organic matter into amino acids that are important for the bacteria life cycle in SSF.

Biological layer formation also includes particle sedimentation and microbial catabolism, when the influent water reaches the filter. Biofilms rich in bacteroidetes and fungal (i.e. *Cryptomycota*) have been observed in SSF, and they are involved in the complex organic compound degradation (Jones et al., 2011). According to Huisman and Wood (1974), the

conditions inside SSF are not suitable for intestinal bacteria multiplication, as the human body temperature is 37 °C and this bacterium does not survive below 30 °C (i.e. common temperatures in the filter). SSF biofilm also captures target organisms that can serve as food for different life forms (Haig et al., 2015; Huisman and Wood, 1974). Channels inside the biofilm enable locomotion, search for food, reproduction and oxygen capture for the microorganism survival. The biological layer constitutes an aerobic ecosystem, therefore DO levels are critical for its rapid formation (Manz, 2004).

HSSF shows the highest efficiency when the biofilm has been formed (ripe filter), however the biofilm changes, reducing the treatment efficiency if the water remains stagnant inside the unit for a long time (Fewster et al., 2004; Souza Freitas and Sabogal-Paz, 2019). An important effect of HSSF biofilm formation is the increase in head loss with a consequent decrease in the treated water production over time. Suspended material contained in the influent water and EPSs obstruct the interstices of the filter bed, reducing the filtration run time and, consequently, increasing the cleaning frequency (Souza Freitas and Sabogal-Paz, 2019). The cleaning procedure takes place to recover treated water production, however this causes a drop in the filter efficiency as it needs to form the biofilm again.

1.3. Microsensors

A microsensor is a small electrochemical electrode used in laboratories for chemical species detection. Its small dimension offers advantages, such as the slight sample volume required, high spatial resolution (< 20 µm), great response speed (< 1.0 s), low sensitivity to stirring, and non-intrusive analysis, therefore it is suitable for biofilm studies and small biological samples.

Biofilm microbiological activity, hydrodynamics and mass transport cannot be analysed separately due to their diverse interactions in the biological layer. The microscale biofilm activity is quantified by microsensor, thus a particular chemical species movement from the substrate to the biofilm surface is analysed. Chemical species movement must be quantified on the spot by microsensors to obtain microprofiles, which ensure adequate spatial distribution with no damage to the biofilm structure under study (Lewandowski & Boltz, 2011). Microsensors are important tools for biofilm analyses, since they provide access to microenvironments with chemical species quantification, on a microscale with high spatial distribution (Lewandowski & Beyenal, 2007).

Most microsensors applied to biofilm analysis are electrochemical and the most used are amperometric, which can measure the dissolved gas concentration, ions, and organic or inorganic molecules. Microsensors can be used in various studies such as blood research, food industry, microbiological corrosion and bioreactor efficiency (Lewandowski & Beyenal, 2007; Revsbech & Jorgensen, 1986; Sarti et al., 2016).

In this context, our study evaluated the C-HSSF and I-HSSF efficiencies to reduce physical-chemical (i.e. turbidity and colour) and microbiological (i.e. total coliforms and *Escherichia coli*) parameters. In addition, temperature, pH, DO and electrical conductivity variations were studied over time. The DO depletion (difference between initial DO concentration and lowest measured concentration) in the non-woven blanket installed on the surface of the fine sand layer was also evaluated to understand the role of the blanket in increasing the filter efficiency, as described by Maciel and Sabogal-Paz (2020).

2. MATERIALS AND METHODS

2.1 HSSFs Characteristics

Two HSSFs of 250 mm internal diameter (0.049 m^2 surface area) were built in PVC, based on the Terin and Sabogal-Paz (2019) model, with adaptations (Figure 1).
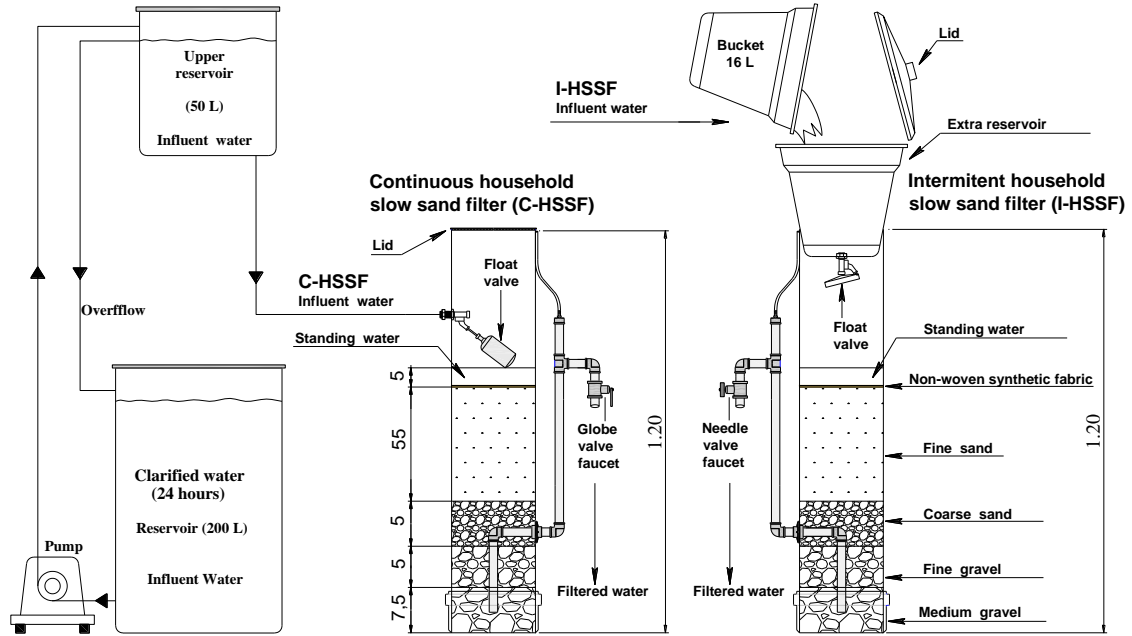

Figure 1. HSSF cross section (units in centimetres)

The filter bed consisted of 55 cm fine sand layer (effective size = 0.15 mm, uniformity coefficient = 1.68 and porosity = 45%). The support layer had 5 cm of coarse sand (1.5-3 mm), 5 cm of fine gravel (5-8 mm) and 7.5 cm of medium gravel (12-15 mm). Sand and gravel were previously washed with groundwater, sun dried and sieved. A non-woven blanket was installed on the fine sand top ($\pm$ 0.2 g cm^{-3} specific weight, 100% polyester and 2 mm thickness) to facilitate the filter cleaning. Non-woven blanket samples to be analysed by microsensors were removed weekly by an exclusive device made of 48 mm diameter PVC discs, attached to the blankets. This device was put back in each HSSF after the microsensor analysis.

2.2. HSSF operation

The HSSFs were continuously operated with water from the Monjolinho River (São Carlos-SP-Brazil) for eight months, between June 2018 and January 2019. A pre-treatment consisting of sedimentation for 24 h and subsequent filtering with a non-woven mat (± 0.2 g cm^{-3}, 100% specific weight, polyester and 2 mm thickness) was applied to reduce the turbidity of the water affluent. The entire set-up of the experimental assembly was kept in a room with controlled temperature (25 °C). Eight filters run took place during the study period, lasting 1 month each. The characteristics of raw and clarified water are shown in Table 1.

Table 1. Characteristics of raw and clarified water quality

Parameter	Raw Water	Clarified water
	Value (M± SD)	Value (M± SD)
Turbidity (NTU)	19.69 ± 21.09	12.8±13.94
Apparent colour (HU)	83.58 ± 55.49	58.95±37.26
True colour (HU)	48.29 ± 33.34	34.28±21.17
pH	6.60 ± 0.17	6.83±0.18
DO (mg L^{-1})	6.33 ± 0.49	6.41±0.48
Electric conductivity (µS cm^{-1})	57.09 ± 8.82	54.1±8.28
Total coliforms (CFU 100 mL^{-1})	7062 ± 3331	5744±4322
E. coli (CFU 100 mL^{-1})	371 ± 799	207±294
Temperature (°C)	20.8 ± 1.9	21.6±1.2

Notes: M: mean; SD: standard deviation

The clarified water was stored in a 200 L tank, and 48 L were pumped daily into an elevated reservoir (50 L) next to C-HSSF (Figure 1). A submersible pump (Jeneca

Electromechanical Co., Ltd., Hong Kong) in the 200 L tank kept the water level constant in the elevated reservoir, which had one overflow connector. The 50L reservoir outlet and the C-HSSF inlet were connected by hoses (the inlet was equipped with a float valve for level control and, consequently, the maximum hydraulic load was fixed at 10 cm).

C-HSSF was operated at a $0.90 \pm 0.8 m^3 m^{-2} day^{-1}$ filtration rate (0.04 L min^{-1}) and controlled by a needle valve installed in the filtered water outlet tube. The I-HSSF filtration rate ranged from $8.81 \pm 0.3 m^3 m^{-2} day^{-1}$ (0.03 L min^{-1}) immediately after feeding and reset to zero when the minimum water level inside the filter had been reached.

I-HSSF had a 20 L bucket at the top and a small float-type valve at the bottom (Figure 1). Moreover, 48 L from the 200 L clarified water tank were used for daily manual feeding of this filter. The float controlled the maximum level of water inside the unit. This filter was fed three times a day (08:00 am, 12:00 pm, and 05:00 pm). In each feed, 16 L were transferred with the aid of a plastic bucket (Figure 1). Adopting these feeding schedules resulted in two pause periods (4 h among successive feedings and 12 h between the last feed of the day and the first feed of the following day).

2.3. Tracer tests

The filters' flow characterisation was performed in triplicate, from inserting 100 mL^{-1} of a sodium chloride solution (NaCl) used as a tracer, as described by Terin and Sabogal-Paz (2019). Prior to each test, the filters were cleaned with groundwater until the tracer solution from the previous test had been completely removed.

A conductivity probe (Vernier Software & Technology, USA) was installed at the output of the HSSFs for measuring electrical conductivity in real-time. The previous probe

calibration promoted a correlation between conductivity variation and tracer concentration. Excel 2016 (Microsoft, USA) and Origin 8.6 (OriginLab, USA) processed the data obtained.

I-HSSF was first fed with a 16 L of NaCl solution. The filtration rate dropped to zero at the minimum level of operation and, at that moment, 16 L groundwater feeding was performed. This last feeding was repeated twice. Data were collected and the graphics obtained were analysed according to the proposals put forward by Bradley (2011) and Elliott et al (2008). The data collection happened when the tracer started its exit from the filter.

The tracer was applied in the C-HSSF as a step input, as recommended by Levenspiel (1999) and Terin and Sabogal-Paz (2019). The filtration rate was maintained at 0.90 $m^3m^{-1}day^{-1}$ (0.04 L min^{-1}) throughout the tests. Concentration curves in relation to time (C vs t) were plotted and the hydraulic retention time (HRT) was estimated. The flow was characterised according to the dispersion models (low and high), number of reactors in series (N-CSTRs) and dispersion index (MDI), as described by Tchobanoglous et al. (2003).

2.4. Sample collection and analysis

Samples of raw, clarified, and filtered water were collected daily to assess the turbidity and apparent colour, and weekly for measurements of pH, DO, true colour, electrical conductivity, total coliforms, and *E. coli*. The protocols established in APHA et al. (2012) were followed for the analyses. The filtered water samples from the C-HSSF were collected daily at 10:00 am, and those from the I-HSSF were obtained after the longest break (12 hrs) at 09:00 am.

Analyses by Clark-type (<20μm) polarographic microsensors were performed weekly on the non-woven blanket, therefore each filter run generated 4 DO microprofiles. The microsensors were constructed from platinum (50 µm diameter) and silver (200 µm diameter)

wires, as described in Lamon et al. (2008). The internal components of platinum and silver enabled us to obtain reference electrodes (Ag/AgCl anodes), and the body was constructed from glass Pasteur pipettes (Figure 2).
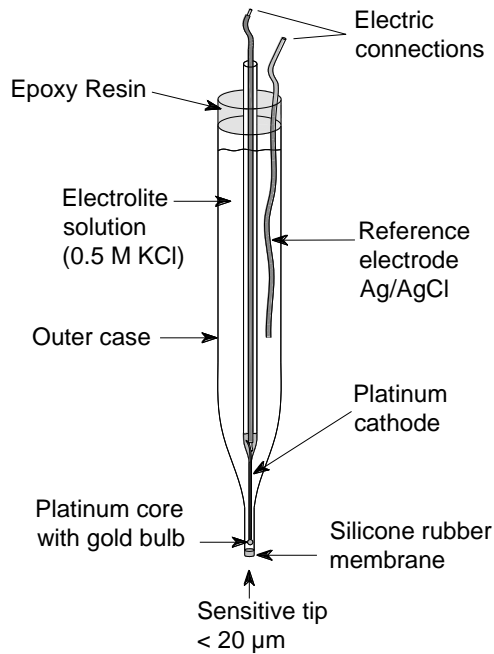

Figure 2. DO microsensor and components.

The microsensors were manually constructed in the laboratory before the measures. The measures were destructive to the microsensor (i.e., it was used and discarded); consequently, each sample collection was time consuming and laborious. Hence, the sample data collection of DO by microsensors was limited to one event per week, which demanded preparation from previous days.

Since DO microsensors offer a linear response, two reading points were used for calibration. The first was obtained with oxygen saturated water (DO saturated according to temperature and local atmospheric pressure = 7.8 mg L^{-1}), and the second was achieved in a sodium sulfite solution (5%), corresponding to the zero DO value.

A data acquisition system was developed specially for application in LabView® language. The microsensors were vertically introduced into the non-woven blanket samples by

a micro-stepper, also controlled by software. The microsensor position (depth in µm), which appears on the X axis, and the DO concentration at 1 pps (point per second) acquisition speed and 20 µm spatial resolution, visualised on the Y axis, were obtained in the DO microprofiles.

The maintenance of the HSSFs was performed every 30 days and it consisted of removing the non-woven blankets and their washing with groundwater. Afterwards, the blankets were reinstalled and a new filter run began. The sand layer, below the blanket, was not agitated or cleaned.

2.5. Statistical analysis

The one-way ANOVA statistical test evaluated the DO depletion in the blankets of C-HSSF and I-HSSF and the removal efficiency. The Mann-Whitney (two samples) statistical test was applied for *E. coli* and total coliforms data by PAST® software Version 2.17c (Baschart/Boxplot) (Palaeontological Statistics) developed by Hammer et al. (2018), with a $p<0.05$ significant difference.

## 3.   RESULTS AND DISCUSSION

3.1. HSSF Design

The HSSF model studied had identical geometry and characteristics to those presented in Andreoli and Sabogal Paz (2020), Freitas et al. (2021) and Terin et al (2021). The I-HSSF and C-HSSF body weight was 13 kg and 12.4 kg, respectively. For the sake of comparison, the concrete HSSF model of the Centre for Affordable Water and Sanitation Technology – CAWST had a structural weight of 95 kg (CAWST, 2009). In addition to the advantage of having less weight, the HSSF model adopted in the present study overcomes issues such as

cracks and leaks, which are occurrences to which the concrete model is more susceptible.

(Earwaker and Webster, 2009).

3.2. Tracer tests

The tracer concentration ranged from 0 mg L^{-1} to 98 mg L^{-1} throughout the tests (Figure 3 a, b). Figure 3a shows the pattern of increase and decrease in tracer concentration, a result similar to that reported by Bradley et al. (2011), Maciel and Sabogal-Paz (2020), Sabogal-Paz et al. (2020), and Terin and Sabogal-Paz (2019). The difference in the pattern of the tracer exit between I-HSSF and C-HSSF should be noted. In the intermittent unit, the assay was conducted with pure water feeding after the tracer feeding. The pure water output pattern was observed in the second half of this assay, after 300 minutes.

The tracer assay in the C-HSSF was conducted differently to obtain flow index presented below and to calculate the HRT. The HRT is essential when working with continuous feed to have a more precise comparison between influent and treated water.
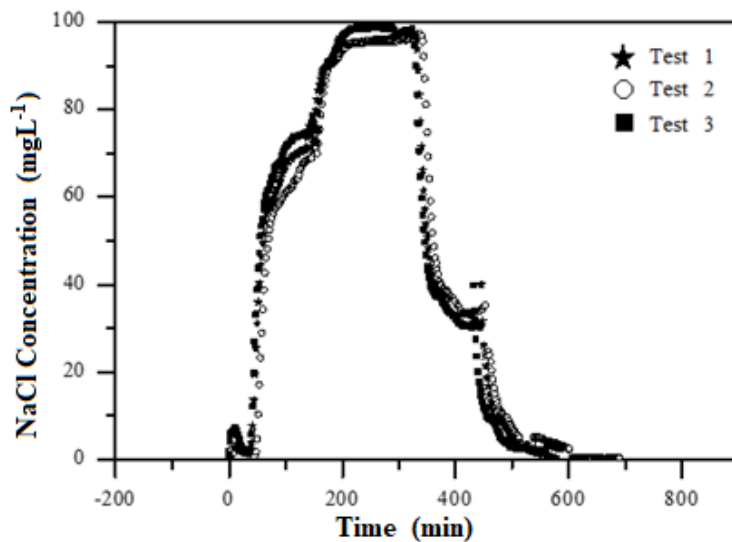
a) I-HSSF
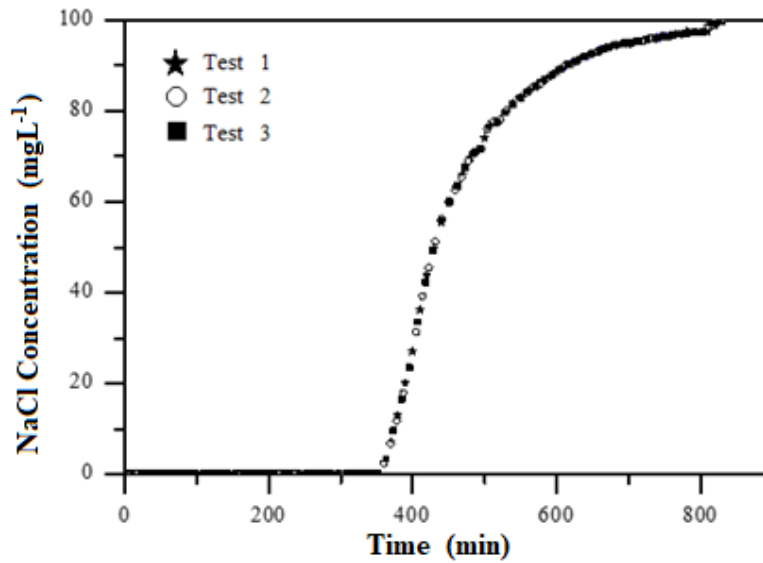
b) C-HSSF

Figure 3. Tracer test results for I-HSSF(a) and C-HSSF (b) (assays in triplicate).

The MDI of the C-HSSF was 1.87 ± 0.04, which is slightly higher than that reported by Elliott et al. (2008) with 1.3 MDI, and Bradley et al. (2011) with a 1.4 MDI, however the MDI obtained (≤ 2.0) characterises the filter as a plug-flow reactor, according to the classification established by USEPA (1986) and Tchobanoglous et al. (2003).

The 464 min ± 42.66 HRT for C-HSSF was used to collect the filtered water samples to evaluate their efficiency. The N-CSTR model best fitted the flow characteristics with $r^2 = 0.66$ and N = 21. According to Levenspiel (1999), the higher the N value, the closer the reactor to the plug-flow model. Sabogal-Paz et al. (2020) reported lower N (17) and higher r^2 (0.75), operating C-HSSF for a daily production of 2.9 ± 0.9 L. The result of the C-HSSF modelling based on ideal extremes is shown in Table 2.

Table 2. Tracer test results for C-HSSF.

Statistic	HRT	N-CSTR	Small dispersion	High dispersion

				model		model	
		N	r^2	D/uL	r^2	D/uL	r^2
Mean	464	21	0,66	0,024	0,57	0,022	0,62
Standard deviation	1,16	0,24	0,005	0,0003	0,005	0,0003	0,006

Notes: HRT: hydraulic retention time; N-CSTR: N-Continuous stirred tank reactor model; N: number of stirred tank reactors; r^2: coefficient of determination; D/µL: the dimensionless group that characterises the spread in the whole reactor (close to zero denotes negligible dispersion, hence the plug flow reactor).

From the perspective of the development of the biological layer and removal processes in slow sand filters, a plug-flow reactor suggests the same time is available for all water parcels that enter the HSSF, thus helping the water treatment (Sabogal- Paz et al., 2020).

3.3. HSSF Operation

Eight filter runs lasting 1 month each were obtained, regardless of the HSSF clogging level. HSSF ripening occurs slowly and requires approximately 1 month for maximum efficiency (CAWST, 2012). The formation of the biological layer increased the filtration head loss and reduced the filtration rate. The quality of the filtered water over the 8 months of operation is shown in Table 3. It showed improved water quality over time, as reported by Ho et al. (2007) and Grützmacher et al. (2002).

Table 3. Filtered water quality and removal or variation rates for I-HSSF and C-HSSF.

Parameter	C-HSSF	I-HSSF	*p-*

	Value (M ± SD)	Removal (R) or variation (V) (%) (M ± SD)	Value (M ± SD)	Removal (R) or variation (V) (%) (M ± SD)	value
Temperature (°C)	23.3 ± 1.5	1.6 ± 6.8(V)	22.6 ± 1.4	1 ± 6.5(V)	3.53
pH	7.1 ± 0.2	0.3 ± 1(V)	6.9 ± 0.2	0.1±1(V)	0.008 SS
DO (mg L^{-1})	5.6±0.6	0.7±11.5(V)	5.7 ± 0.6	0.7±11(V)	0.826
Electrical Conductivity (µS cm^{-1})	53.0 ± 7.1	-1.2±2.2% (V)	53.1 ± 7.3	-1.1 ± 2(V)	0.953
Turbidity (NTU)	3.0 ± 3.9	75.9±31.1(R)	3.2 ± 4.1	74.8 ± 32.1(R)	0.744
Apparent colour (uH)	15.7±16.8	73.4±28.5(R)	16.1±15.5	72.8 ± 26.4(R)	0.834
True colour (uH)	14.5±16.0	57.5±46.8(R)	16.2±16.7	52.7 ± 48.9(R)	0.52
Total coliform (CFU 100 mL^{-1})	33 ± 46	1.6 Log ± 0.04 log	45 ± 67	1.4 Log ± 0.06 log	0.714

E.coli (CFU 100 mL^{-1})	1 ± 1	2.2 log ± 1 log	3 ± 3	1.6 log ± 0.01 log	0.02 SS

M: mean; SD: standard deviation; statistically significant difference (SS) between C-HSSF and I-HSSF when *p*-value < 0.05.

Regarding turbidity removal, no statistically significant difference was observed between C-HSSF and I-HSSF ($p = 0.744$). Removals in the 70% to 96% range in laboratory and field trials have been reported (CAWST, 2012; Frank et al., 2014; Jenkins, 2011), therefore the expected removal efficiency was obtained. Results of turbidity removal in HSSF operations whose influent water has higher levels of turbidity are enhanced (Napotnik et al., 2017; Tundia et al., 2016; Nair et al., 2014). However, another tendency was observed in the present study. An improved turbidity removal rate was observed in the second month of operation (91.8% ± 0.14 for C-HSSF and 87.1% ± 0.36 for I-HSSF), when the mean value of clarified water was 4.43 ± 0.76 NTU. In the fifth month, higher turbidity of the influent was observed, 33.7 ± 25.4 NTU, with removal rates of 83.6% ± 7.2 for C-HSSF and 82.9% ± 7.2 for I-HSSF, values similar to those reported by Jenkins (2011) and Frank et al. (2014). Water produced by both HSSFs showed average turbidity values below the maximum limit accepted of 5.0 NTU, recommended by the World Health Organization (WHO, 2017).

The greatest efficiency of apparent colour removal was achieved in the second month of operation with 92.2% ± 1.35 for I-HSSF and 87.9% ± 2.45 for C-HSSF. Ellis and Wood (1985) reported that slow sand filtration is a process in which low removal of humic substances occurs from raw water. No significant difference was perceived in the apparent colour produced by I-HSSF and C-HSSF ($p = 0.8345$). In the second month, the removal of true colour was 80.6% ± 1.8 for C-HSSF and 81.8% ± 0.57 for I-HSSF, with no significant

difference between I-HSSF and C-HSSF ($p = 1$). The average true colour value of both I-HSSF and C-HSSF was near the limit of 15 HU established by the World Health Organization (WHO, 2017).

In the water produced by the HSSFs, the mean pH value of the affluent (6.83 ± 0.18 pH) increased to 7.1 ± 0.2 pH for C-HSSF and 6.9 ± 0.2 pH for I-HSSF, due to the contact of the water with the filter medium (Sabogal-Paz et al. 2020). A significant difference was observed between the filters ($p = 0.008$).

Regarding electrical conductivity, the mean value of the influent water in 8 months of operation was 54.2 ± 8.28 µS cm^{-1}. Filtered water produced by C-HSSF and I-HSSF showed average values of 53.00 ± 7.11 µS cm^{-1} and 53.09 ± 7.36 uScm^2, respectively, which is similar to the value of influent water. The leaching effect of the filter bed did not lead to effective increase conductivity, as observed by Sabogal-Paz et al. (2020), who used an effluent with low concentrations of mineral ions to feed the HSSFs. No significant difference was detected between the HSSFs ($p = 0.768$).

As shown in Table 2, the reductions in total coliforms were 1.6 ± 0.4 log for C-HSSF and 1.4 ± 0.06 log for I-HSSF, nonetheless no statistically significant differences were observed between the filters ($p = 0.714$). The reductions in *E.coli* were 2.2 ± 1 log for C-HSSF and 1.6 ± 0.01 log for I-HSSF, with a significant difference between the filters ($p = 0.02$).

The lower filtration rate in C-HSSF favoured the *E. coli* reduction compared to the I-HSSF. This result is in accordance with previous studies which compared performance between continuous and intermittent filters (Maciel and Sabogal-Paz, 2020; Young-Rojanschi and Madramootoo, 2014). The importance of the filtration rate was highlighted in the study of Freitas et al. (2021) in which no difference was found in evaluated parameter efficiencies between continuous HSSF with the same filtration rate and different media depth.

The average reduction of *E. coli* was similar to that observed in other studies (Elliott et al., 2008; Kennedy et al., 2013; Stauber et al., 2006). Although the total coliforms and *E. coli* in the filtered water were counted, the C-HSSF model presented protected efficiencies (> 2.0 log) against bacteria (WHO, 2014). Nevertheless, it would be desirable to perform post-treatment disinfection in terms of meeting the World Health Organization guidelines (WHO, 2017). WHO (2017) recommends the direct measurement of disinfectant residual as a warranty of water quality, rather than bacterial count.

The decays in dissolved oxygen in relation to the influent water observed in the filtered water were 11.45% ± 0.83 for C-HSSF and 10.97% ± 0.70 for I-HSSF. These reductions were associated with both actions of microorganisms in their metabolic activities and chemical action of the substrate (Taft et al., 1980). No significant difference was observed in the DO reduction between the HSSFs ($p = 0.8266$).

3.4. Dissolved Oxygen microprofiles

DO microprofiles obtained from the non-woven blanket of I-HSSF and C-HSSF throughout the months showed a similar trend, therefore only those obtained in the first month are presented (Figure 4).
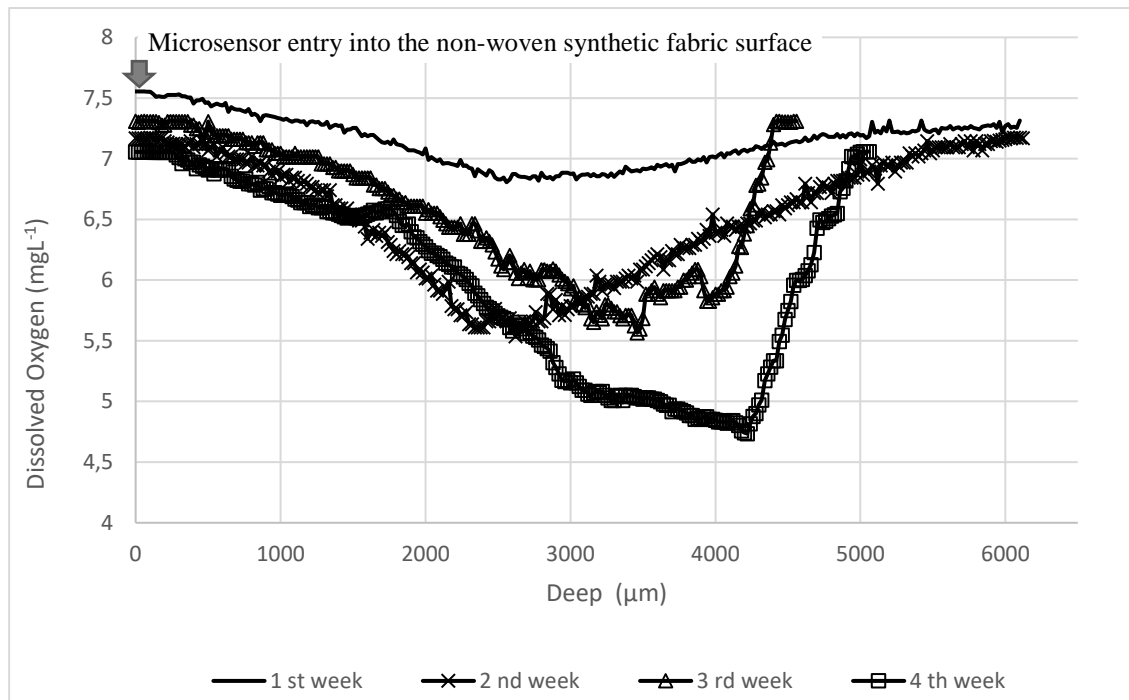
a) DO microprofile of non-woven synthetic fabric installed in C-HSSF in a filter run period.
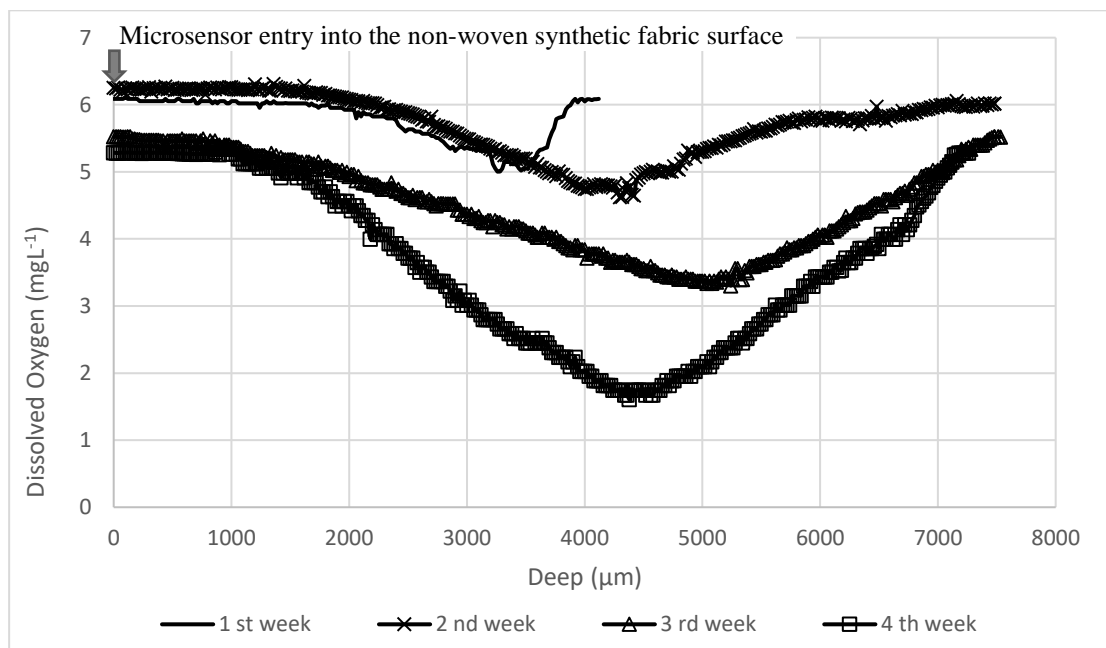
b) DO microprofile of non-woven synthetic fabric installed in I-HSSF in a filter run period.

Figure 4. DO microprofile of non-woven synthetic fabric installed in the HSSFs. At the beginning and at the end of each profile, DO concentrations are the same and correspond to the immersion water concentration of the samples.

The microsensors measured the entire thickness of the blanket samples, and at the beginning and end of each microprofile, the DO values were almost the same. They are relatively stable values, because they are measurements obtained in the immersion liquid (water) that is on and under the samples, where the action of biofilms is not effectively observed (Sarti et al., 2016; Lewandowski & Boltz, 2011).

The maximum values of DO depletion were obtained near the bottom of the blanket samples, which are in contact with the surface of the HSSF filter bed. No anaerobic region was observed in the microprofiles, as the measurements were maintained above 1.0 mg L^{-1}. Low DO concentrations limit the biofilm development (Donlan, 2002).

DO measurements taken by microsensors revealed the absence of a first inflection point, which might determine the biofilm surface (boundary layer) (Lewandowski et al., 1990) for assisting the effective measurement of the biological layer thickness. However, the presence of DO concentration gradients was observed. Their depletion is relatively low, when compared to the microprofiles obtained in biofilms adhered to media applied to the treatment of wastewater (for example). A rapid DO decay is observed from the boundary layer, in some cases anoxia at the base of the biofilms (Sarti et al., 2016).

Figure 5 shows the relationship between the HSSF progressive efficiency increase in the removal of turbidity and the progressive increase in the DO depletion in non-woven blankets during the first month of operation. In this period, the mean turbidity removal was 83.10% ± 0.82 for C-HSSF and 80.00% ± 1.30 for I-HSSF.
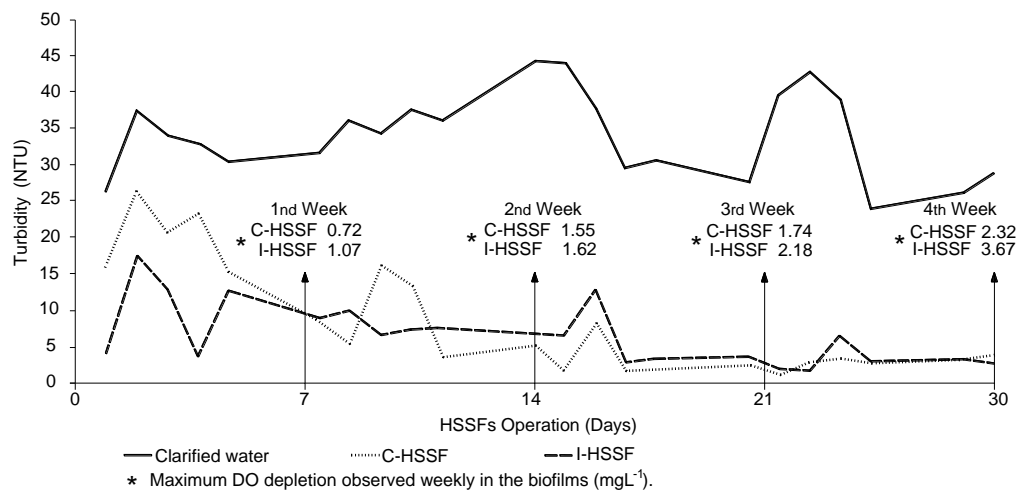
Figure 5. The relation between Maximum DO depletion observed in the non-woven synthetic fabric samples for C-HSSF and I-HSSF and turbidity.

In the last measurement of the first filter run (fourth week), the DO depletion was observed in the blanket of 2.32 mg L^{-1} and 3.67 mg L^{-1}, respectively for C-HSSF and I-HSSF. The intermittency condition in the hydraulic flow could have influenced the way the particulate material suspended in the liquid medium is sedimented on the blankets, thus influencing the mass transfer on a microscale (Lewandowski & Boltz, 2011). More prominent biofilms collaborated positively to the result of HSSFs (drinking water production), obtained over the time of operation in a process known as HSSF ripening (CAWST, 2012).

DO gradients in biofilms adhered to HSSFs have not been investigated by microsensors, however, according to Ranjan & Prem (2018), organic matter together with microorganisms in a liquid medium rich in dissolved oxygen is a favourable environment for biofilm formation. Therefore, the DO depletion observed in the HSSF blanket samples is directly related to the respiration of microorganisms in their metabolic activities (Ranjan & Prem, 2018) and the chemical action of particulate matter deposited on the non-blanket samples by the affluent water (Taft et al., 1980), such as mineral crystals, corrosion particles, clay or mud particles (Donlan, 2002).

The increasing supply of suspended material contained in the liquid medium, together with the accumulation of EPSs produced by microorganisms in their metabolic activities lead to a natural filling of HSSFs, characterised by increased pressure loss, which decreases both water production and diffusivity of dissolved oxygen in the biofilm (Logsdon et al., 2002). Since most of the slow sand filtration is expected to be conducted by a wide range of microorganisms (Wakelin et al., 2011), the progressive depletion of DO observed can limit the microbiological development, restricting access from active biota to oxygen from water (Ranjan & Prem, 2018).

There were no differences in DO depletion in the non-woven synthetic fabric between I-HSSF and C-HSSF considering the 8 months of operation ($p = 0.98$). The values were respectively, 1.88 ± 0.90 mg L^{-1} and 1.87 ± 0.56 mg L^{-1}. It was expected that there would be greater oxygen depletion in the I-HSSF, since the water remained at rest for the 12-hour pause period in this unit.

Young-Rojanschi and Madramootoo (2014) observed lower DO concentration on the top of the intermittent filter with a 24-hour pause period compared to the continuous filter. Young-Rojanschi and Madramootoo (2014, 2015) used sensors installed on the side of the filter to measure DO. They admitted that the absence of sensors immediately in the schmutzdecke when discussing the data was a limitation of the study. In contrast, microsensors used in our study were able to perform DO measurements with precision and spatial distribution of the entire non-woven synthetic fabric thickness.

4. CONCLUSIONS

DO microprofiles obtained in the non-woven blanket revealed the presence of gradients of dissolved oxygen, intensified during the time of operation by the biofilm development. Therefore, the process ripening progressively restricts the penetration of dissolved oxygen into

biofilms, and consequently the HSSF efficiency increases. Statistical analyses of the maximum oxygen depletion values showed no significant difference between the HSSFs studied.

No anaerobic region was observed in the DO microprofiles of both C-HSSF and I-HSSF.

No significant differences between C-HSSF and I-HSSF efficiencies were found, except for *E.coli*, which showed a greater reduction in the C-HSSF. Both C-HSSF and I-HSSF produced water with turbidity and true colour near or slightly higher than the limit value established by WHO. Regarding bacterial parameters, the reduction achieved by the C-HSSF above 2 *E. coli* log classifies the model as a protective technology.

More research is necessary for a better understanding of the role of the biological layer and its relationship with dissolved oxygen to increase the filtered water quality.

5. ACKNOWLEDGEMENTS

6. DATA AVAILABILITY STATEMENT

The authors confirm that the data supporting the findings of this study are available within the article. The raw data that support the findings of this study are available on request from the corresponding author.

7. REFERENCES

APHA, AWWA, WEF 2012. Standard Methods for Examination of Water and Wastewater, 22ª
ed. American Public Health Association, Washington, ISBN 978-087553-013-0, p. 1360.

Andreoli, F. C., & Sabogal-Paz, L. P. 2020. Household slow sand filter to treat groundwater
with microbiological risks in rural communities. Water Research, 116352.
https://doi.org/10.1016/j.watres.2020.116352

Bradley, I., Straub, A., Maraccini, P., Markazi, S., Nguyen, T.H. 2011. Iron oxide amended
biosand filters for virus removal. Water Res. 45, 4501e4510. https://
doi.org/10.1016/j.watres.2011.05.045.

Buzunis, B. J. 1995. *Intermittently operated slow sand filtration: a new water treatment
process*. Civil Engineering, University of Calgary.

Centre for Affordable Water and Sanitation Technology (CAWST). 2009. Biosand filter
manual design, construction, installation, operation and maintenance. A CAWST training
manual Calgary (AB): Centre for Affordable Water and Sanitation Technology.

Centre for Affordable Water and Sanitation Technology (CAWST). 2012. Biosand filter
construction manual. Calgary (AB): Centre for Affordable Water and Sanitation
Technology.

Clair C. 2009. "Biosand filtration of high turbidity water: Modified filter design and safe
filtrate storage" Thesis submitted to the Department of civil and Environment
Engineering in Partial fulfillment of the requirements for the degree of Master of
Engineering in Civil and Environmental Engineering at Massachusetts Institute of
Technology.

Donlan, R. M. 2002. Biofilms: Microbial Life on Surfaces. Centers for Disease Control and
Prevention, Atlanta, Georgia, USA. Emerging Infectious Diseases. Vol. 8, No. 9.

Earwaker, P., & Webster, J. (2009). Evaluation of the long term sustainability of biosand filters

    in rural Ethiopia. Water, Sanitation and Hygiene: Sustainable Development and

    Multisectoral Approaches - Proceedings of the 34th WEDC International Conference

Elliott, M. A.; Stauber, C. E.; Koksal, F.; DiGiano, F. A.; Sobsey, M. D. 2008. Reductions of

    E-coli, Echovirus type 12 and bacteriophages in an intermittently operated household-

    scale slow sand filter. Water Res. 2008; 42:2662–2670.

EPA 2015. Office of Web Communications and Office of Environmental Information. Point of

    Use (POU) Technologies Radionuclides Decision Tree US EPA. Available in:

    http://cfpub.epa.gov/safewater/radionuclides/radionuclides.cfm?action=Rad_Point%20of

    %20Use (accessed 27 February 2015).

Fewster, E.; Mol, A.; Wiessent-Brandsma, C. 2004. The Bio-sand Filter. Long-term

    sustainability: user habits and technical performance evaluated. Presentation given at the

    2003 International Symposium on Household Technologies for Safe Water, 16–17 June,

    2004, Nairobi, Kenya.

Frank, T.E.; Scheie, M.L.; Cachro, V.; Muñoz, A.S. 2014. The effect of increasing grain size in

    biosand water filters in combination with ultraviolet disinfection. J. Water Sanit Hyg.

    Dev. 4 (2), 206–213. https://doi.org/10.2166/washdev.2013.171.

Freitas, B.L.S., Terin, U.C., Fava, N. de M.N., Sabogal-Paz, L.P., 2021. Filter media depth and

    its effect on the efficiency of Household Slow Sand Filter in continuous flow. J. Environ.

    Manage. 288, 112412. https://doi.org/10.1016/j.jenvman.2021.112412

Gottinger, Ann; M. Dena; W. Mcmartin; Doug Price; and Bruce Hanson. 2011. The

    effectiveness of slow sand filters to treat Canadian rural prairie water. Published by NRC

    Research Press. Can. J. Civ. Eng. 38: 455–463.

Grützmacher, G., Böttcher, G., Chorus, I., Bartel, H., 2002. Removal of microcystins by slow

    sand filtration. Environ. Toxicol. 17, 386e394. https://doi.org/10.1002/tox.10062.

Haig, S.J.; Schirmer, M., D'amore, R.; Gibbs, J.; Davies, R.L.; Collins, G.; Quince, C. 2015. Stable-isotope probing and metagenomics reveal predation by protozoa drives E. coli removal in slow sand filters. ISME 9:797–808.

Hall-Stoodley, L., Costerton, J.W., Stoodley, P. 2004. Bacterial biofilms: from the natural environment to infectious diseases. Nat. Rev. Microbiol. 2 (2), 95. https://doi.org/10.1038/nrmicro821.

Hammer, O., Harper, D.A., Ryan, P.D. 2018. PAST3 palaeontological statistics, ver. 3.22 Paleontological. Museum, University of Oslo, Norway.

Ho, L., Hoefel, D., Saint, C.P., Newcombe, G. (2007). Degradation of microcystin-LR through biological sand filters. Pract. Period. Hazard. Toxic, Radioact. Waste Manag. 11, 191e196. https://doi.org/10.1061/(ASCE)1090-025X(2007)11:3(191).

Huisman, L., and Wood, W. E. 1974. *Slow sand filtration* (Vol. 16). Geneva: World Health Organization.

Jenkins, M.W.; Tiwari, S.K.; Darby, J. 2011. Bacterial, viral and turbidity removal by intermittent slow sand filtration for household use in developing countries: Experimental investigation and modeling. Water Res. 45, 6227–6239. https://doi.org/10.1016/j.watres.2011.09.022.

Jones, M.D.; Forn, I.; Gadelha, C.; Egan, M.J.; Bass, D.; Massana, R.; Richards, T.A. 2011. Discovery of novel intermediate forms redefines the fungal tree of life. Nature 474:200-203.

Kennedy, T.J.; Hernandez, E.A.; Morse, N.A.; Anderson, T.A. 2012. Hydraulic loading rate effect on removal rates in a bioSand filter: a pilot study of three conditions. Water Air Soil Pollut. 2012;223(7):4527–4537.

Kennedy TJ, Anderson TA, Hernandez EA, et al. 2013. Determining the operational limits of the biosand filter. Water Sci Technol Water Supply. 2013;13(1):56–65. doi: 10.2166/ws.2012.075

Kristina, R.; Pfannes & Kilian M. W. Langenbach & Giovanni Pilloni & Torben Stührmann & Kathrin Euringer & Tillmann Lueders & Thomas R. Neu & Jochen A. Müller & Matthias kästner & Rainer U. Meckenstock 2015. Selective elimination of bacterial faecal indicators in the Schmutzdecke of slow sand filtration columns. Appl Microbiol Biotechnol (2015). 99:10323–10332.

Lamon, A. W.; Gonzalez, B. C.; Sati, A.; Campos, J. R. 2008. Advanced system for growth evaluation of aerobic/anaerobic biofilm through the use of microsensor. XXXI Congreso Interamericano AIDIS Santiago – Chile Centro de Eventos Casa Piedra 12 – 15.

Levenspiel, O. 1999. Chemical Reaction Engineering, Industrial & Engineering Chemistry Research. https://doi.org/10.1021/ie990488g.

Lewandowski, Z.; Walser, G.; Larsen, R.; Peyton, B. and Characklis, W.G. 1990. Biofilm surface positioning. Environmental engineering proceedings 1990, EE Div/ASCE, Arlington, VA, July, 1990, 17.

Lewandowski, Z. & Beyenal, H. 2007. Fundamentals of Biofilm Research. Book. CRC Press. 6000 Broklen Sound Parkway NW, Suit 300. Boca Raton. ISBN: 0-8493-3541-8, p.28.

Lewandowski, Z. and Boltz, J. 2011. Biofilms in Water and Wastewater Treatment. Elsevier B.V. 2011. DOI: 10.1016/B978-0-444-53199-5.00095-6.

Logsdon, G. S., Kohne, R., Abel, S. & LaBonde, S. 2002. Slow sand filtration for small water systems. J. Enviorn. Eng. Sci. 1(5), 339–348.

Maciel, P. M. F., Sabogal-Paz, L. P., 2020. Household slow sand filters with and without water level control: continuous and intermittent flow efficiencies. Environmental technology, *41*(8), 944-958. https://doi.org/10.1080/09593330.2018.1515988

Mahaffy, N. C.; Dickson, S.; Cantwell, R. E.; Lucier, k. and Schuster-Wallace, C. J. 2015. Effects of physical disturbances on media and performance of household-scale slow sand (BioSand) filters. IWA Publishing 2015. Journal of Water Supply: Research and Technology – AQUA, 64.3.

Manz, D. 2004. New Horizons for Slow Sand Filtration Published in the Proceedings of the Eleventh Canadian National Conference and Second Policy Forum on Drinking Water and the Biennial Conference of the Federal-Provincial-Territorial Committee on Drinking Water, Promoting Public Health through Safe Drinking Water, April 3–6, 2004, Calgary, Alberta; 2004; 682–92.

Nair, A. T.; Ahammed, M. M.; Davra, K. 2014. Influence of operating parameters on the performance of a household slow sand filter. Water Science and Technology-Water Supply, v. 14, n. 4, p. 643-649.

Napotnik, J. A.; Baker, D.; Jellison, K. L. 2017. Effect of Sand Bed Depth and Medium Age on Escherichia coli and Turbidity Removal in Biosand Filters. Environmental Science & Technology, v. 51, n. 6, p. 3402-3409.

Pfannes, K. R.; Langenbach, K. M. W.; & Pilloni, G.; Stührmann, T.; Euringer, K.; Lueders, T.; Neu, T. R.; Müller, J. A.; kästner, M.; Meckenstock, R. U. 2015. Selective elimination of bacterial faecal indicators in the Schmutzdecke of slow sand filtration columns. Appl Microbiol Biotechnol (2015) 99:10323–10332.

Ranjan, P., & Prem, M. (2018). Schmutzdecke- A Filtration Layer of Slow Sand Filter. International Journal of Current Microbiology and Applied Sciences, 7(07), 637–645.

Revsbech, N. P. (1989). An oxygen microsensor with a guard cathode. Limnol. Oceanogr. 34 (2), 474–478.

Revsbech, N. P. and Jorgensen, B. B. 1986. Microelectrodes: their use in microbial ecology. Adv. Microb. Ecol. 9, 293-352.

Sabogal-Paz, L. P.; Campos, L. C.; Bogush; A.; Canales, M. 2020. Household slow sand filters in intermittent and continuous flows to treat water containing low mineral ion concentrations and Bisphenol A. Science of the Total Environment 702(2020)135078. https://doi.org/10.1016/j.scitotenv.2019.135078.

Saravanan, S.P. and Gobinath, R. 2015. Drinking Water Safety through Bio Sand Filter - A Case Study of Kovilambakkam Village, Chennai. International Journal of Applied Engineering Research, ISSN 0973-4562 Vol. 10 No.53.

Sarti, A.; Lamon, A. W.; Ono, A. and Foresti, E. 2016. A new device to select carriers for biomass immobilization and application in an aerobic/anaerobic fixed-bed sequencing batch biofilm reactor for nitrogen removal. Water Science & Technology, 74.11.

Schmidt, W.P., Cairncross, S., 2009. Household water treatment in poor populations: is there enough evidence for scaling up now? Environ. Sci. Technol. 43 (4), 986–992. https://doi.org/10.1021/es802232w.

Shaikh, I. and Munavalli, G.R. 2015. Modified Biosand Filter–A Review. Journal of Civil Engineering and Environmental Technology Print ISSN: 2349-8404; Online ISSN: 2349-879X; v 2, n 4.

Sianipar, C.P.M.; Yudoko, G.; Dowaki, K.; Adhiutama, A. 2013. Design methodology for appropriate technology: Engineering as if people mattered. *Sustainability* **2013**, *5*, 3382–3425.

Souza Freitas, B.L., Sabogal-Paz, L.P., 2019. Pretreatment using *Opuntia cochenillifera* followed by household slow sand filters: technological alternatives for supplying isolated communities. Environ. Technol. 1–12. https://doi.org/10.1080/09593330.2019.1582700.

Stauber, C.E.; Elliott, M.A.; Koksal, F.; Ortiz, G.M.; Digiano, F.A.; Sobsey, M.D. 2006. Characterisation of the biosand filter for *E. coli* reductions from household drinking water

under controlled laboratory conditions and field use conditions. Water Sci. Technol., 54 (3) (2006), pp. 1-7

Taft, L. L.; Taylor, W.; Hartwig, E. O.; Loftus, R. 1980. Seasonal Oxygen Depletion in Chesapeake Bay JAY L. Estuaries Research Federation. Vol. 3, No. 4, p. 242-247.

Tchobanoglous, G., Burton, F.L., Stensel, H.D., 2003. Wastewater Engineering: Treatment and Reuse. McGraw-Hill Higher Education, New York.

Terin, U.C., Sabogal-Paz, L.P. 2019. Microcystis aeruginosa and microcystin-LR removal by household slow sand filters operating in continuous and intermittent flows. Water Res. 150, 29–39. https://doi.org/10.1016/j.watres.2018.11.055.

Terin U.C., Freitas, B. L.S., Fava, N. M. N., Sabogal-Paz, L. P. 2021. Evaluation of a multi-barrier household system as an alternative to surface water treatment with microbiological risks. Environ. Technol., DOI: 10.1080/09593330.2021.1921856

Tundia, K. R.; Ahammed, M. M.; George, D. 2016. The effect of operating parameters on the performance of a biosand filter: a statistical experiment design approach. Water Science and Technology-Water Supply, v. 16, n. 3, p. 775-782.

United States Environmental Protection Agency. 1986. Municipal Wastewater Disinfection. Design Manual EPA/625/1-86/021. Cincinatti, Ohio, 247 pp.

United States Environmental Protection Agency. 2006. Point-of-Use or Point-of- Entry Treatment Options for Small Drinking Water Systems. EPA 815-R-06-010. Arlington, VA, 132 pp.

Wakelin, S.; D. Page, P. Dillon, P. Pavelic, G. C. J. Abell, A. L. Gregg, E. Brodie, T. Z. Desantis, k. C. Goldfarb and G. Anderson 2011. Microbial community structure of a slow sand filter schmutzdecke: a phylogenetic snapshot based on rRNA sequence analysis. IWA Publishing 2011 Water Science & Technology: Water Supply, 11.4.

World Health Organization (WHO), 2014. An international scheme to evaluate household

water treatment technologies. World Health Organization, Geneva, Switzerland.

World Health Organization (WHO) 2015. The United Nations children fund. Key facts from

JMP 2015 Report. Available from:

http://www.who.int/water_sanitation_health/publications/JMP-2015-keyfacts-en-

rev.pdf?ua=1 .

World Health Organization (WHO) 2017. The United Nations children's fund. Progress on

drinking water, sanitation and hygiene: 2017 update and SDG baselines. Geneva: World

Health Organization (WHO) and the United Nations Children's Fund (UNICEF).

Young-Rojanschi, C., Madramootoo, C. 2015. Comparing the performance of biosand filters

operated with multiday residence periods. J. Water Supply Res. Technol. 64, 157.

https://doi.org/10.2166/aqua.2014.027.

Young-Rojanschi, C.; Madramootoo, C. 2014. Intermittent versus continuous operation of

biosand filters. Water Res. 2014; 49:1–10.